

# Alterations in Burst Firing of Thalamic VPL Neurons and Reversal by Na v1.3 Antisense After Spinal Cord Injury

Bryan C. Hains, Carl Y. Saab and Stephen G. Waxman

*J Neurophysiol* 95:3343-3352, 2006. First published Feb 15, 2006; doi:10.1152/jn.01009.2005

**You might find this additional information useful...**

---

This article cites 50 articles, 14 of which you can access free at:

<http://jn.physiology.org/cgi/content/full/95/6/3343#BIBL>

Updated information and services including high-resolution figures, can be found at:

<http://jn.physiology.org/cgi/content/full/95/6/3343>

Additional material and information about *Journal of Neurophysiology* can be found at:

<http://www.the-aps.org/publications/jn>

---

This information is current as of September 7, 2006 .

# Alterations in Burst Firing of Thalamic VPL Neurons and Reversal by Na<sub>v</sub>1.3 Antisense After Spinal Cord Injury

Bryan C. Hains,<sup>1,2</sup> Carl Y. Saab,<sup>3</sup> and Stephen G. Waxman<sup>1,2</sup>

<sup>1</sup>Department of Neurology and Center for Neuroscience and Regeneration Research, Yale University School of Medicine, New Haven;

<sup>2</sup>Rehabilitation Research Center, Veterans Affairs Connecticut Healthcare System, West Haven, Connecticut; and <sup>3</sup>Department of Surgery, Rhode Island Hospital, Brown University School of Medicine, Providence, Rhode Island

Submitted 26 September 2005; accepted in final form 7 February 2006

**Hains, Bryan C., Carl Y. Saab, and Stephen G. Waxman.** Alterations in burst firing of thalamic VPL neurons and reversal by Na<sub>v</sub>1.3 antisense after spinal cord injury. *J Neurophysiol* 95: 3343–3352, 2006. First published February 15, 2006; doi:10.1152/jn.01009.2005. We recently showed that spinal cord contusion injury (SCI) at the thoracic level induces pain-related behaviors and increased spontaneous discharges, hyperresponsiveness to innocuous and noxious peripheral stimuli, and enlarged receptive fields in neurons in the ventral posterolateral (VPL) nucleus of the thalamus. These changes are linked to the abnormal expression of Na<sub>v</sub>1.3, a rapidly repriming voltage-gated sodium channel. In this study, we examined the burst firing properties of VPL neurons after SCI. Adult male Sprague–Dawley rats underwent contusion SCI at the T9 level. Four weeks later, when Na<sub>v</sub>1.3 protein was upregulated within VPL neurons, extracellular unit recordings were made from VPL neurons in intact animals, those with SCI, and in SCI animals after receiving lumbar intrathecal injections of Na<sub>v</sub>1.3 antisense or mismatch oligodeoxynucleotides for 4 days. After SCI, VPL neurons with identifiable peripheral receptive fields showed rhythmic oscillatory burst firing with changes in discrete burst properties, and alternated among single-spike, burst, silent, and spindle wave firing modes. Na<sub>v</sub>1.3 antisense, but not mismatch, partially reversed alterations in burst firing after SCI. These results demonstrate several newly characterized changes in spontaneous burst firing properties of VPL neurons after SCI and suggest that abnormal expression of Na<sub>v</sub>1.3 contributes to these phenomena.

## INTRODUCTION

Experimental spinal cord injury (SCI) produces behaviors indicative of chronic neuropathic pain (Hains et al. 2001; Hulsebosch et al. 2000), concomitant with development of hyperresponsiveness in spinal cord dorsal horn nociceptive neurons (Hains et al. 2003a,b, 2004) and in higher-order neurons of the ventral posterolateral (VPL) nucleus of the thalamus (Hains et al. 2005). Most dorsal horn nociceptive neurons project rostrally to the contralateral VPL, which is involved in sensory-discriminative aspects of pain (Price and Dubner 1977; Willis and Coggeshall 2004). Pain-related changes in thalamic structure and functional properties have been documented in rats (Gerke et al. 2003), subhuman primates (Weng et al. 2000), and humans (Apkarian et al. 2004; Lenz et al. 1989, 1994; Pattany et al. 2002), with electrophysiologic changes including the emergence of burst firing (Gerke et al. 2003; Lenz 1989, 1994; Weng et al. 2000).

Factors underlying abnormal thalamic electrophysiology after SCI are only partially understood. We have recently demonstrated that in a rodent model of SCI, neurons of the VPL develop high-frequency spontaneous activity, become hyperresponsive to peripheral stimulation, produce afterdischarges, and have larger peripheral receptive fields (Hains et al. 2005). Increased spontaneous discharge activity persists after spinal cord transection rostral to the lesion, indicating that the thalamus develops independent hyperexcitability after SCI. At the same time, the Na<sub>v</sub>1.3 sodium channel is abnormally expressed within VPL neurons after SCI, and intrathecal administration of antisense (AS) oligodeoxynucleotides generated against Na<sub>v</sub>1.3 reverses these electrophysiologic changes. Na<sub>v</sub>1.3 repriming (recovers from inactivation) rapidly and produces a depolarizing current in response to small stimuli close to resting potential, thus increasing the excitability of cells in which it is expressed (Cummins and Waxman 1997; Cummins et al. 2001).

We have proposed that hyperresponsive dorsal horn neurons produce an increased spinal barrage that triggers molecular changes in thalamic nuclei that process and relay nociceptive inputs (Hains et al. 2005), that could help to maintain chronic pain after SCI, independent of spinal activity. Consistent with this hypothesis, spinal cord transection (Melzack and Loeser 1978) and conduction block (Loubser and Donovan 1991), rostral to the site of SCI, are ineffective in eliminating pain in humans after SCI, suggesting that the thalamus can serve as an abnormal central pain generator, independent of pathological drive from spinothalamic neurons (Waxman and Hains 2006).

In this study, we hypothesized that thalamic VPL neurons manifest abnormal burst firing properties after SCI. Our analysis revealed that there are changes in a number of burst features after injury and suggest that the Na<sub>v</sub>1.3 sodium channel contributes to these phenomena.

## METHODS

### *Animal care*

Experiments were carried out in accordance with National Institutes of Health guidelines for the care and use of laboratory animals; all animal protocols were approved by the Yale University Institutional Animal Use Committee. Adult male Sprague–Dawley rats (200–225 g) were used for this study. Animals were housed under a 12-h light–dark cycle in a pathogen-free area with free access to water and food.

Address for reprint requests and other correspondence: S. G. Waxman, Department of Neurology, LCI-707, Yale School of Medicine, 333 Cedar Street, New Haven, CT 06510 (E-mail: stephen.waxman@yale.edu).

The costs of publication of this article were defrayed in part by the payment of page charges. The article must therefore be hereby marked “advertisement” in accordance with 18 U.S.C. Section 1734 solely to indicate this fact.

### Spinal cord contusion injury

Rats were deeply anesthetized with ketamine/xylazine [80/5 mg/kg, administered intraperitoneally (ip)]. Spinal contusion injury ( $n = 22$ ) was produced at spinal segment T9 using the MASCIS/NYU impact injury device (Gruner 1992), whereby a 10-g, 2.0-mm-diameter rod was released from a 25-mm height onto the exposed spinal cord. For sham surgery, animals ( $n = 7$ ) underwent laminectomy and placement into the vertebral clips of the impactor without impact injury. After SCI or sham surgery ("intact" group), the overlying muscles and skin were closed in layers with 4–0 silk sutures and staples, respectively, and the animal was allowed to recover on a 30°C heating pad. Postoperative treatments included saline [2.0 ml, administered subcutaneously (sc)] for rehydration and Baytril (0.3 ml, 22.7 mg/ml sc, twice daily) to prevent urinary tract infection. Bladders were manually expressed twice daily until reflex bladder emptying returned, typically by 10 days postinjury. After surgery, animals were maintained under the same preoperative conditions and fed without restriction.

### Oligodeoxynucleotide synthesis and delivery

In animals ( $n = 15$ ) 28 days after SCI, under ketamine/xylazine (80/5 mg/kg, ip) anesthesia, a sterile premeasured 32G intrathecal (i.t.) catheter (ReCathCo, Allison Park, PA) was introduced through a slit in the atlantooccipital membrane, threaded down to the lumbar enlargement, secured to the neck musculature with suture, and heat sealed to prevent infection and leakage of cerebrospinal fluid. Three days after catheter placement (day 31 after SCI), under brief (<1 min) halothane sedation (3% by facial mask), i.t. administration of an antisense (AS) oligodeoxynucleotide (ODN) sequence corresponding to the translation initiation site of Na<sub>v</sub>1.3 (5'-CAG TGC CTG GGC CAT CTT TTC-3') ( $n = 7$ ) or its mismatch (MM, 5'-CGA TCG CGT GCG CTA TCT TCT-3') ( $n = 8$ ) was initiated (see Hains et al. 2004, 2005). For 4 days, 45  $\mu$ g/5  $\mu$ l twice daily of either AS or MM in artificial cerebrospinal fluid (aCSF; 1.3 mM CaCl<sub>2</sub> · 2H<sub>2</sub>O, 2.6 mM KCl, 0.9 mM MgCl, 21.0 mM NaHCO<sub>3</sub>, 2.5 mM Na<sub>2</sub>HPO<sub>4</sub> · 7H<sub>2</sub>O, 125.0 and mM NaCl, prepared in sterile H<sub>2</sub>O) was injected followed by 10  $\mu$ l aCSF flush. On day 4 of ODN administration (day 34 after SCI), Cy3-tagged AS or MM was delivered in the same manner to a subset of these animals. By a search using the Basic Local Alignment Search Tool (<http://www.ncbi.nlm.nih.gov/BLAST/>; Altschul et al. 1990), the antisense sequence did not show similarity, over the entire 21 nucleotides, to the sequences for any other sodium channel or to other genes.

### Electrophysiological procedures

Animals from control intact, SCI, SCI + MM, and SCI + AS groups underwent extracellular single-unit recording of VPL neurons according to established methods (Hains et al. 2005). SCI animals were studied from 4 to 5 wk after injury. The activity of four to seven units/animal were recorded, yielding 28–56 units/group. Rats were initially anesthetized with halothane (4% in induction chamber) and maintained by tracheal intubation (1.1%, 2–2.5 ml tidal volume, 60–70 strokes/min). Rectal temperature was maintained at 37°C. The head was fixed in a stereotaxic apparatus (Kopf Instruments, Tujunga, CA) and a skin incision was made with a minimal craniotomy to allow electrode penetration. The recording microelectrode was mounted on a hydraulic microdrive (Kopf Instruments) for accurate vertical migration and electronic display of travel distance.

Neuronal units were isolated from the ventral posterolateral (VPL) nucleus of the thalamus (stereotaxic coordinates in mm: bregma [−3.14]; lateral [2.0–3.5]; vertical [5.0–7.0]). Extracellular single-unit recordings were made with a low-impedance 5-M $\Omega$  tungsten-insulated microelectrode (A-M Systems, Carlsborg, WA). Electrical signals were amplified and filtered at 300–3,000 Hz (DAM80, World Precision Instruments, Sarasota, FL), processed by a data collection

system (CED 1401+; Cambridge Instruments, Cambridge, UK), and stored on a computer (Latitude D800, Dell, Austin, TX) with Spike2 software (v5.03, Cambridge Electronic Design, Cambridge, UK). Once a cell was identified, its receptive field was mapped and it was classified as a multireceptive unit according to previously referenced methods (Hains et al. 2005). Spike2 template-matching routines and principal component analysis were used to differentiate among multiple units in wavemark records.

Records of burst firing were obtained in the absence of peripheral receptive field stimulation for periods of  $\leq 600$  s. Burst analysis was performed using the Spike2 burstsv1.25.s2s script (<http://www.ced.co.uk/sp2wptu.shtml#bursts>) and burst events were identified by the following parameters: maximum interval signifying burst onset (6 ms), maximum interspike interval (9 ms), longest increase in interspike interval within a burst (2 ms), and minimum number of spikes within a burst (2). Burst events were examined statistically and burst duration, interspike interval, interburst interval, and events per burst versus time were computed. Histograms showing distribution of spikes/burst, burst duration, and interburst intervals were constructed. In addition, interspike interval durations were plotted against number of spikes contained within a burst and linear regression analysis was performed on the duration of first interspike intervals versus number of interspike intervals per burst from these data. Unit firing modes were categorized as silent, single-spiking, bursting, or spindle waves (identified by firing frequency [intra-sequence frequency of 7–14 Hz, intersequence frequency of about 0.2 Hz], waxing and waning amplitude, duration of more than 2 s, full return to baseline between spindle waves, and shape). A burst epoch was defined as a period of sustained firing of bursts for more than 2 s, where each burst was separated by <300 ms from one burst to the next burst. Phase histograms were constructed from records containing burst epochs. To analyze the relative contributions of discrete frequencies to signal, fast Fourier transformation (FFT) of waveform data into power (frequency) spectra was performed. FFT block size was set to 1,024 (512 bins at 97.66 Hz) as determined by Nyquist criteria, with Hanning windowing of root mean square data.

At the conclusion of recording, a direct current (1  $\mu$ A for 20 s) was passed through the recording electrode to identify the location of unit recording sites. Recording sites were plotted from three to four animals in each group: intact ( $n = 3$ ), SCI ( $n = 4$ ), and SCI + AS ( $n = 3$ ). The brain was removed and fixed in 4% cold buffered paraformaldehyde in PBS for 48 h at 4°C in 30% sucrose before frozen sectioning at 20  $\mu$ m. Sections were mounted on gelatin/potassium chromium sulfate-coated slides and stained with cresyl violet (0.1%) for visualization and photomicroscopy.

### Statistical analysis

All statistical tests were performed at the alpha level of significance of 0.05 by two-tailed analyses using parametric tests. Data were tested for significance using one-way ANOVA to determine degree of variability within a sample and whether there was a difference between groups among the obtained means, followed by Bonferroni post hoc analysis. Tests of factors including pairwise comparisons were performed with either the paired Student's *t*-test for before–after comparisons or the two-sample Student's *t*-test to compare two groups. Data management and statistical analyses were performed using SAS (1992) statistical procedures with SigmaStat (v1.0) and graphed using SigmaPlot (v7.0) as mean  $\pm$  SD.

## RESULTS

### Recording sites

Coronal histological sectioning through the ventrobasal nucleus complex of the thalamus corresponding to bregma −3.14 mm confirmed that the tip of the recording electrode was

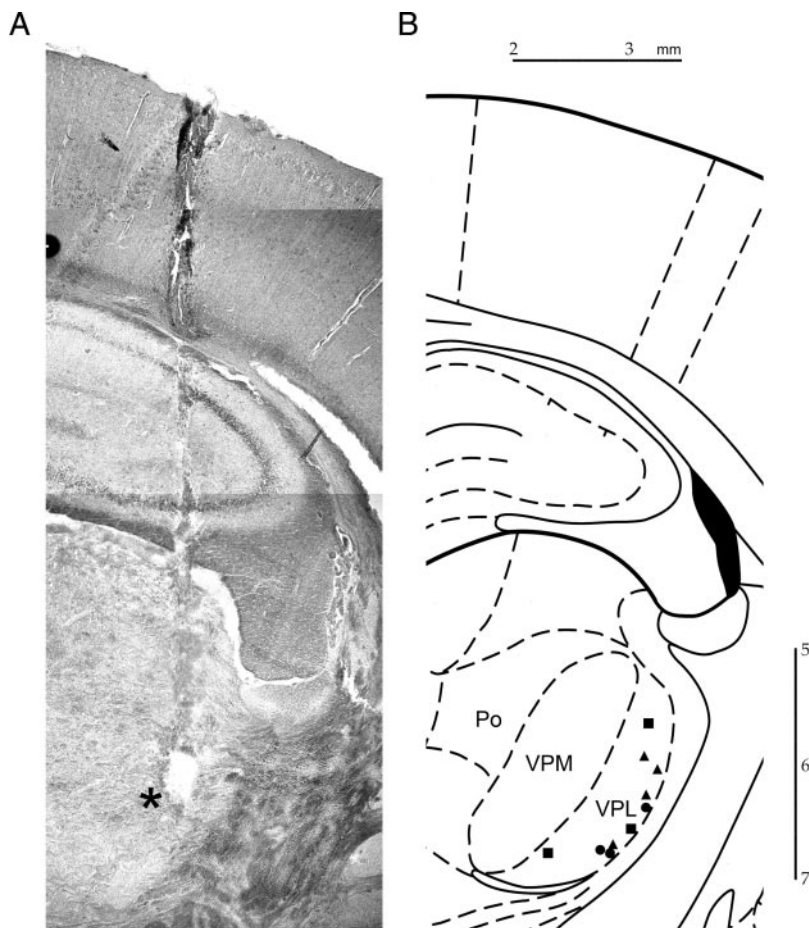


FIG. 1. Photomontage of a coronal section through the brain corresponding to bregma  $-3.14$  mm, showing electrode penetration through the cortex and hippocampus, with termination (asterisk) and lesioning in the ventral posterolateral (VPL) nucleus of the thalamus (A). Two-dimensional distribution of 10 histologically identified recording sites plotted on a schematic diagram (Paxinos and Watson 1998) of the ventrobasal complex of the thalamus, which delineates the posterior nucleus group (Po), ventral posteromedial nucleus (VPM), and VPL. Units from intact (circles), spinal cord contusion injury (SCI) (squares), and SCI + antisense (AS) (triangles) groups are shown. All units used in this analysis were confined to the VPL.

within the VPL. A typical electrode penetration is shown in Fig. 1A. The track of the electrode passed through the hippocampus and VPM and, in this case, ended in the VPL. Superimposed on a schematic diagram of the ventrobasal complex of the thalamus (Paxinos and Watson 1998) is the distribution of histologically identified electrode lesions marking 10 recording sites (Fig. 1B). All units analyzed were contained within the atlas boundaries of the VPL. Aberrant expression of the  $\text{Na}_v1.3$  sodium channel (which is not detectable within the thalamus of intact animals) within VPL neurons after SCI is documented in Hains et al. (2005) and is not illustrated here.

#### Burst epochs

In intact animals, epoch firing was observed in 13% of units sampled, compared with 33% of units sampled in animals with SCI. In units from intact animals, the mean epoch duration was  $4.9 \pm 2.3$  s ( $n = 15$  units) (Fig. 2C). InterePOCH intervals ranged from 4.6 to 8.0 s (mean  $6.5 \pm 1.2$  s). In SCI animals, the mean epoch duration was  $8.7 \pm 2.8$  s ( $n = 18$  units) (Fig. 2C), and interepoch intervals ranged from 2.3 to 5.4 s (mean  $4.0 \pm 1.1$  s). A typical epoch pattern in a unit after SCI is shown in Fig. 2A, with epochs of different lengths labeled *a* and *b*. In this case, each epoch had a unique duration. Phase histograms of two different units (Fig. 2B) demonstrate epochs of variable length in records of 366 s (Fig. 2Ba) and 420 s (Fig. 2Bb) lengths. Spinal administration of  $\text{Na}_v1.3$  AS to SCI

animals did not significantly change the proportion of units that displayed epochs (22% of sampled units), epoch duration ( $7.5 \pm 3.0$  s), or interepoch interval range 2.4–12.5 s (mean  $7.7 \pm 3.2$  s,  $n = 18$  units) (Fig. 2C).

#### Burst analysis

In units from SCI animals, the rate of single-spike events was significantly elevated ( $6.5 \pm 1.5$  spikes/s,  $n = 18$  units analyzed) compared with units from intact animals ( $2.9 \pm 1.0$  spikes/s,  $n = 19$  units analyzed) as shown previously (Hains et al. 2005). Burst firing was present in both groups. To illustrate the differences in single-spike events and burst event firing patterns, representative traces are shown in Fig. 3. In this example, burst activity was random in intact animals (Fig. 3A). In contrast, after SCI, burst events exhibited a rhythmic (oscillatory) firing pattern (Fig. 3B).  $\text{Na}_v1.3$  AS treatment disrupted this oscillatory pattern (Fig. 3C). Expanded sample traces of individual burst events for units from intact, SCI, and SCI + AS animals are shown in Fig. 3, A, B, and C, respectively.

The predominant spike configuration [88% of sampled bursts ( $n = 50$ )] in our records from units from SCI animals was consistent with high-threshold spikes; characterized by discharges without a preburst silent period, an increased number of burst events occurring during epochs of increased firing, and the presence of oscillatory frequencies at 5–10 Hz. In some cases (12%), low threshold spikes characterized by very long preburst interspike intervals were observed.

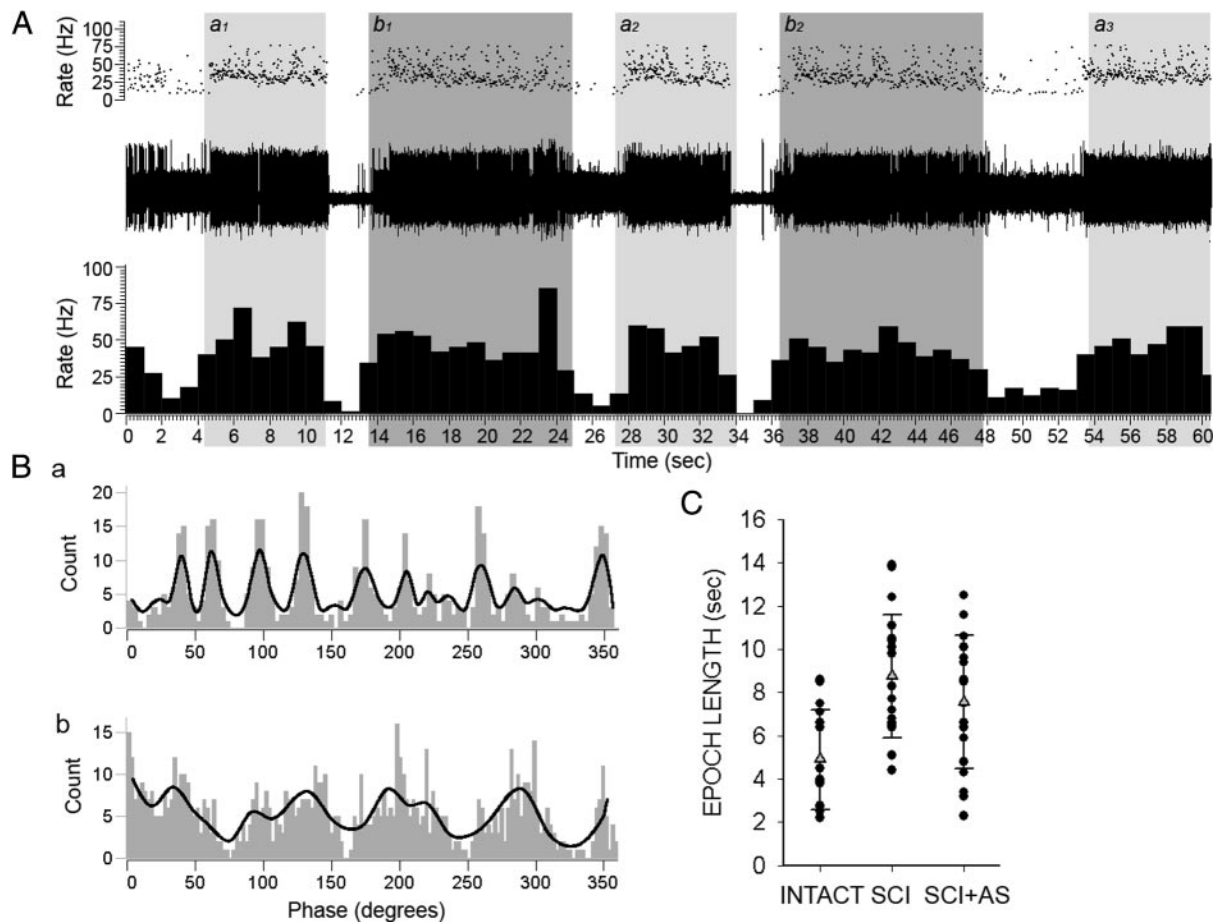


FIG. 2. Periods of sustained burst activity (“epochs”) in a representative VPL unit after SCI (A). In this example, 60 s of spontaneous firing activity was recorded, and 2 alternating burst epochs with unique periods were identified as *a* and *b*. These 2 epochs alternated in a repeated manner and were separated by interepoch intervals of low firing activity. Subsequent epochs are denoted by subscript numbers. Phase histograms constructed from 2 different unit recordings from SCI animals demonstrate distributions of variable period cycles in records of  $4.9 \pm 1.3$  s (Ba) and  $7.6 \pm 1.9$  s (Bb). Compared with units from intact animals, the mean epoch duration was not significantly different in units from that of SCI animals (C).  $\text{Na}_v1.3$  AS administration did not significantly reduce the mean epoch duration after SCI (C).

Power spectrum analysis showed greater oscillatory burst activity in units from SCI and SCI + AS groups, compared with units from the intact group ( $n = 6$  units/group analyzed). In units from intact animals, power amplitudes were dominant at lower frequencies (Fig. 4A) and discrete peaks were present at frequencies within the power spectrum corresponding to spontaneous discharge frequencies ( $2.3 \pm 1.3$  Hz, Fig. 4A). In units from SCI (Fig. 4B) and SCI + AS (Fig. 4C) groups, increases in power amplitudes occurred at higher frequencies, indicative of burst activity ( $2.1 \pm 1.1$  and  $5.0 \pm 1.8$  Hz, and broad peak from 4.3 to 9.7 Hz, Fig. 4B). Delivery of  $\text{Na}_v1.3$  AS did not significantly decrease peak power amplitude or area, and increases in power amplitudes were also observed at  $4.9 \pm 1.8$  Hz (Fig. 4C), although the broad peak was less prominent, suggesting a trend toward reversal to an irregular firing mode.

Burst features are shown in Fig. 5. Representative interval duration histograms showed that in units from intact animals ( $n = 89$  bursts analyzed) (Fig. 5A), spike events occurred with variable interval durations. Higher spike counts were present within several domains on the histogram, the first of which is 0–10 ms, and the second 10–35 ms. After SCI ( $n = 114$  bursts analyzed), spike intervals became oscillatory, as evidenced by the high spike count within a single short interval duration

period (0–10 ms), and not at any other time period (Fig. 5B). Treatment with  $\text{Na}_v1.3$  AS ( $n = 124$  bursts analyzed) caused spike events to assume an irregularly distributed firing pattern (Fig. 5C), similar to the pattern in units from intact animals. There was no difference between SCI and SCI + MM groups (data not shown).

Individual spike events per burst were significantly reduced in units from SCI animals ( $5.1 \pm 1.4$  spikes/burst) (Fig. 5Ba) compared with those in intact animals ( $9.2 \pm 1.1$  spikes/burst) (Fig. 5Aa). After  $\text{Na}_v1.3$  AS treatment, the number of spike events within bursts ( $8.0 \pm 1.5$  spikes/burst) was significantly greater compared with SCI (Fig. 5Ca). Mean burst duration was not significantly different in units from intact animals ( $15.9 \pm 8.0$  ms) (Fig. 5Ab), compared with units from SCI animals ( $11.1 \pm 5.1$  ms) (Fig. 5Bb), or after  $\text{Na}_v1.3$  AS administration ( $12.6 \pm 7.8$  ms) (Fig. 5Cb). Distribution of mean interburst intervals showed no significant differences between intact ( $3.9 \pm 0.9$  ms) (Fig. 5Ac), SCI ( $3.6 \pm 0.7$  ms) (Fig. 5Bc), and SCI + AS ( $3.8 \pm 1.4$  ms) (Fig. 5Cc) groups.

Quantitative analysis of burst duration is summarized in Table 1. Compared with units from intact animals, units from animals with SCI showed significant differences in spikes/burst and burst duration for bursts that contained at least four spikes

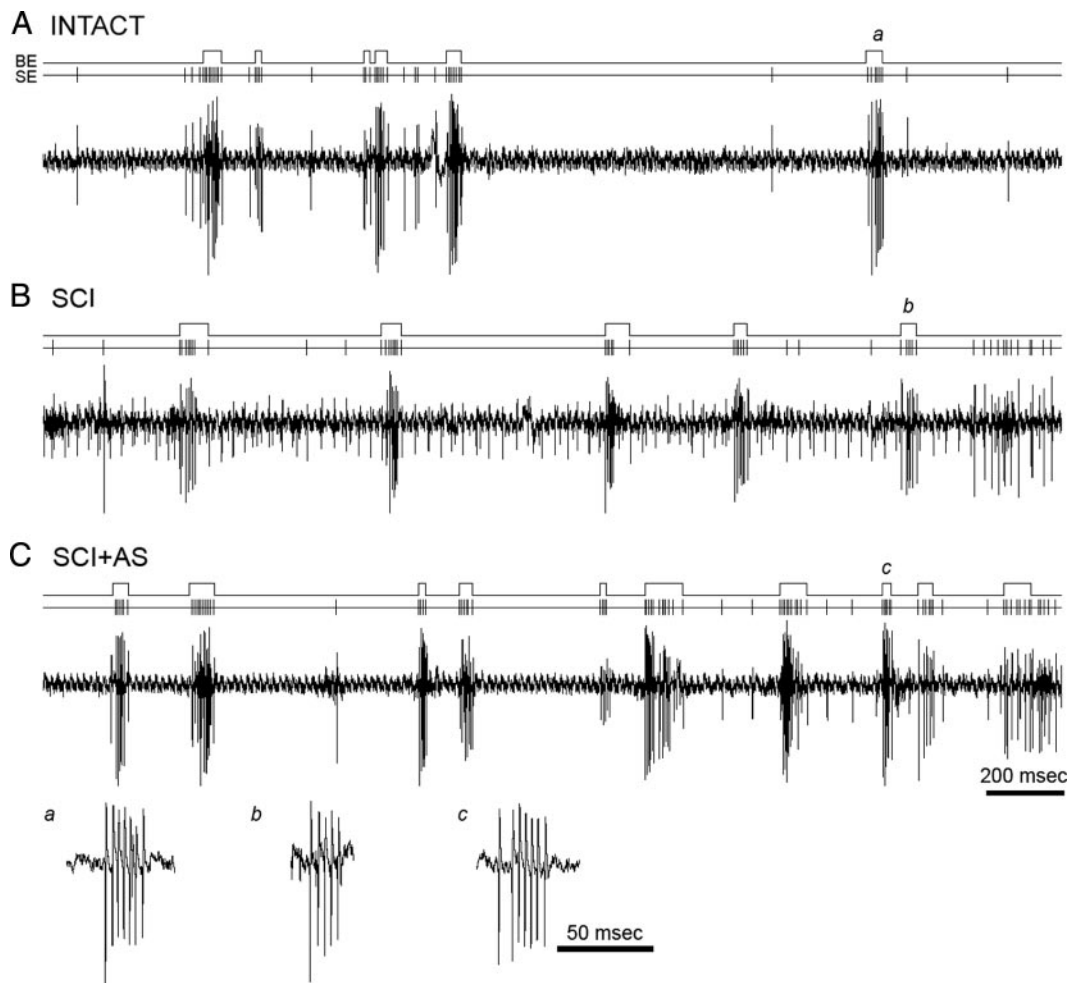


FIG. 3. Representative records of spontaneous firing of VPL units from intact, SCI, and  $\text{Na}_v1.3$  AS-treated animals to illustrate single-spike events (SE) and burst events (BE), denoted above each trace by line deflections. In the unit from the intact group, SE and BE occurrence appeared random (A). In animals with SCI, SE appears random, but BE exhibited a rhythmic oscillatory firing pattern (B). This unit from an SCI animal treated with  $\text{Na}_v1.3$  AS showed a random pattern of SE and BE distribution (C). Individual BEs in units from intact (a), SCI (b), and SCI + AS (c) groups are shown to illustrate the differences in number of discharges per burst and burst duration. After SCI, for example, there were fewer spikes per burst and the burst duration is shorter (b).

(a range of two to seven spikes/burst was analyzed).  $\text{Na}_v1.3$  AS, but not MM, treatment after SCI resulted in a significant reversal in spikes/burst and burst duration for bursts of three, six, and seven spikes only. In units from the SCI group, there

was also a greater decrement in the duration of the first interspike interval compared with the intact group, which became statistically different after four spikes/burst. In units from all three groups of animals, interspike intervals became

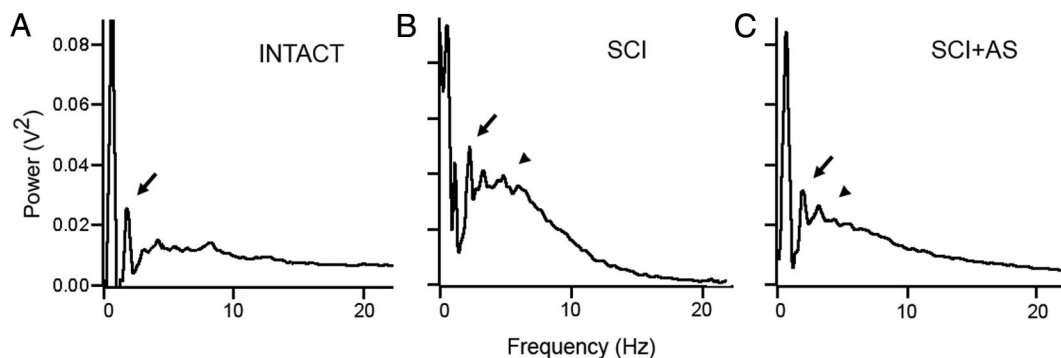


FIG. 4. Power spectrum analysis revealed random burst cycling in units from intact animals, whereas oscillatory burst activity was present in units after SCI and after administration of  $\text{Na}_v1.3$  AS. Representative spectra are shown. In this unit from an intact animal, power amplitudes were dominant at lower frequencies (arrows, A). Discrete peaks were observed within the power spectrum, corresponding to frequencies of spontaneous discharges, but power amplitude was elevated throughout the record. In representative units from SCI (B) and SCI + AS (C) groups, increases in power amplitudes were also observed at relatively higher frequencies (arrowheads), indicative of a greater degree of spontaneous and burst firing. Delivery of  $\text{Na}_v1.3$  AS did not significantly decrease peak power amplitude or power area, although the broad peak suggesting disorganized firing became less prominent.

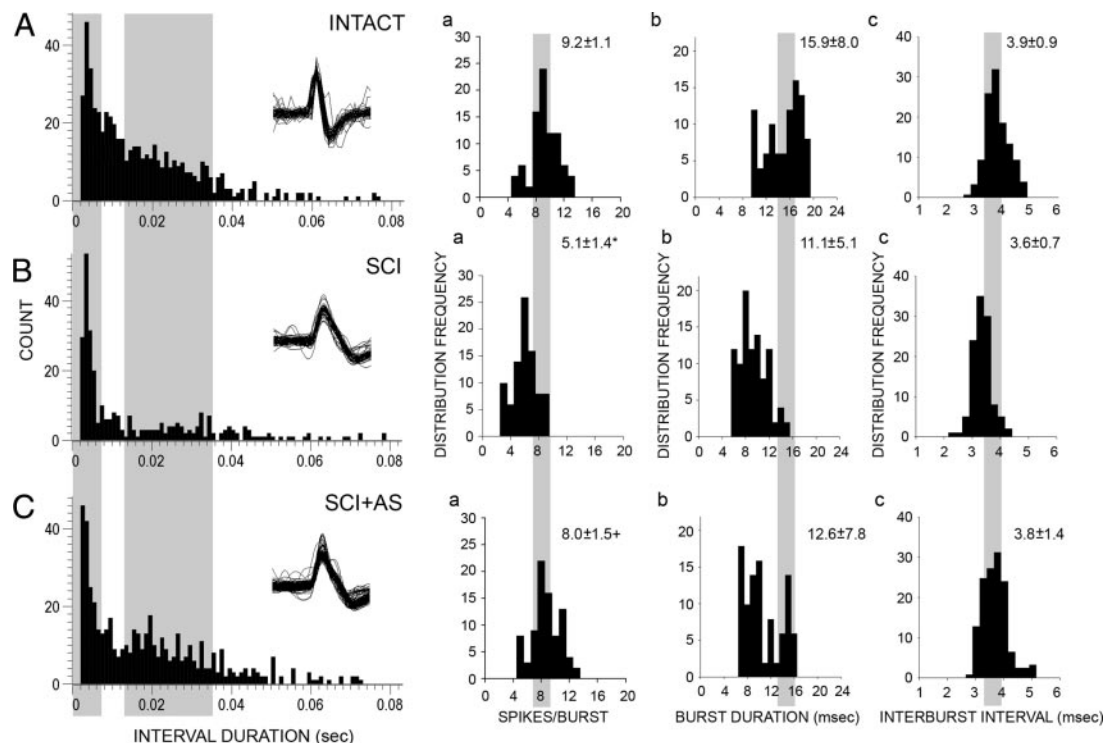


FIG. 5. Features of burst firing in units from intact, SCI, and SCI animals treated with  $\text{Na}_v1.3$  AS are shown in representative interval-duration histograms. In a unit from an intact animal, spike events occurred at irregular intervals (A). After SCI, intervals became more regular, as evidenced by the high spike count within a single interval-duration period (0–10 ms), and not at any other duration period (B). After treatment with  $\text{Na}_v1.3$  AS, spike events became irregularly distributed (C). Wavemark overdraws are shown for each histogram to confirm analysis of single units. Within bursts, units from intact animals exhibited a significantly ( $*P < 0.05$ ) greater number of individual spike events per burst (Aa) when compared with SCI (Ba). In units from SCI animals receiving  $\text{Na}_v1.3$  AS, the number of spike events within bursts was significantly ( $^{\dagger}P < 0.05$ ) reduced (Ca). Units from intact animals (Ab) did not have a significantly longer burst duration than after SCI (Bb).  $\text{Na}_v1.3$  AS administration did not result in a significant increase in burst duration (Cb). Similarly, there were no significant differences in interburst interval in units from intact (Ac), SCI (Bc), and SCI + AS (Cc) groups.

longer with each successive spike in a burst (Fig. 6). For bursts containing increasingly higher numbers of spike events, further interspike interval lengthening was associated with higher burst ordinal, and a deceleration in firing rate throughout the burst was observed. In all groups, an inverse relationship between the first interspike interval duration and the number of spike events per burst was observed; as the number of spike events per burst increased, the duration of the first interspike interval was reduced. Plotting the duration of the first interspike interval against number of intervals per burst illustrated a linear relationship in all groups. The slope function in units from SCI animals was significantly greater ( $y = -0.69x$ ,  $r^2 =$

0.91) (Fig. 6, C and D) compared with units from intact animals ( $y = -0.46x$ ,  $r^2 = 0.90$ ) (Fig. 6, A and B). Administration of  $\text{Na}_v1.3$  AS to SCI animals did not significantly change slope function compared with units from the intact group ( $y = -0.38$ ,  $r^2 = 0.72$ ,  $P = 0.06$ ) (Fig. 6, E and F).

#### Firing modes

A number of sampled units exhibited the ability to spontaneously switch between several unique firing modes (silent, single-spike, burst, spindle waves).

Population analysis of units from intact ( $n = 25$  units), SCI ( $n = 32$  units), and SCI + AS ( $n = 35$  units) groups showed different trends in firing mode distribution. In all groups, discharge activity occurred primarily in single-spike and burst modes. In units from intact animals, where 16% of the units analyzed exhibited alternating firing modes, percentage of time spent in silent, single-spike, burst, and spindle wave modes was 8.3, 47.6, 31.7, and 12.4%, respectively. In units from the SCI group, where 20% of the units analyzed exhibited alternating firing modes, percentage of time spent in silent, single-spike, burst, and spindle wave modes was 3.6, 27.5, 53.8, and 15.1%, respectively. Therefore after SCI, units spent a significantly higher percentage of time in the burst mode and less time in single-spike mode, compared with intact animals.  $\text{Na}_v1.3$  AS did not significantly reverse the shift to a higher percentage of time in burst mode after SCI. In units from SCI + AS animals, where 20% of the units analyzed exhibited

TABLE 1. ISI burst analysis

Property	Group		
	INTACT ( $n = 89$ )	SCI ( $n = 114$ )	SCI + AS ( $n = 124$ )
Burst duration, ms			
2 spikes	$4.9 \pm 0.2$	$4.2 \pm 0.3$	$4.4 \pm 0.2$
3 spikes	$9.8 \pm 0.7$	$8.9 \pm 0.5$	$6.0 \pm 0.3$
4 spikes	$13.7 \pm 0.6$	$9.5 \pm 0.8^*$	$9.9 \pm 1.2$
5 spikes	$18.2 \pm 0.8$	$11.2 \pm 0.7^*$	$12.2 \pm 1.1$
6 spikes	$21.9 \pm 1.4$	$13.1 \pm 1.9^*$	$17.2 \pm 2.3$
7 spikes	$26.8 \pm 1.7$	$19.4 \pm 2.2^*$	$25.7 \pm 2.5^{\dagger}$

Values are means  $\pm$  SD. \*Statistically significant difference between intact and SCI groups ( $P < 0.05$ ).  $^{\dagger}$ Statistically significant difference between SCI and SCI + AS groups ( $P < 0.05$ ).

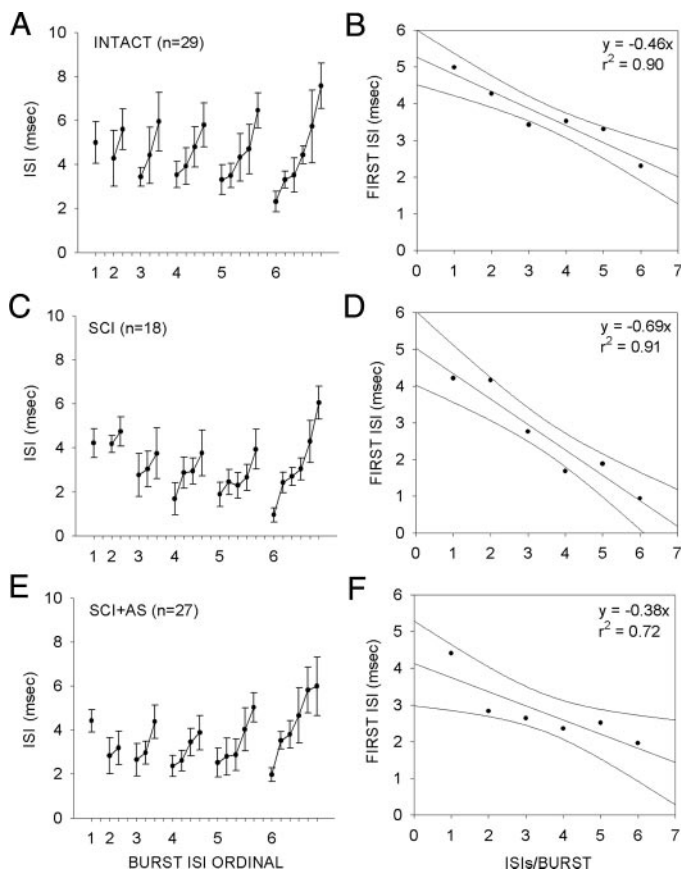


FIG. 6. Interspike interval analysis revealed deceleration of spiking within bursts. In units from intact animals (A), burst length was significantly greater than that for units from SCI (C), and SCI animals treated with  $\text{Na}_v1.3$  AS (E). After SCI, there was a greater decrement in the first interspike interval compared with the intact group. In all groups, an inverse relationship between the first interspike interval and the number of spike events per burst was observed (B, D, F). Compared with units from intact animals (B), SCI units (D) demonstrated a significantly decreased first interspike interval and slope function. Administration of  $\text{Na}_v1.3$  AS (F) resulted in a slope function that more closely approximated the intact group.

alternating firing modes, component percentage of silent, single-spike, burst, and spindle wave modes was 6.2, 44.2, 40.3, and 9.3%, respectively. There was no significant difference between SCI and SCI + MM groups (data not shown).

## DISCUSSION

Dorsal horn nociceptive neurons receive input from the periphery by the dorsal root ganglia and project rostrally to third-order neurons of the ventral posterolateral (VPL) nucleus of the thalamus. This pathway makes up the spinothalamic tract, which mediates pain and thermal signaling (Willis and Coggeshall 2004). Spinal cord injury alters nociceptive processing within both the spinal cord dorsal horn and the VPL, contributing to the development of chronic neuropathic pain in both animal models and humans.

In the current study, we characterized burst firing of VPL neurons after SCI. We report that SCI induces oscillatory burst activity, changes in discrete burst properties, and shifts in the amount of time spent in burst firing mode, concomitant with upregulated expression of the  $\text{Na}_v1.3$  sodium channel. Intrathecal delivery of  $\text{Na}_v1.3$  AS can partially restore thalamic

burst firing properties in SCI animals. These results show that alterations in burst firing properties of VPL neurons after SCI, and arguably nociceptive processing, can be partially reversed by knockdown of abnormal expression of  $\text{Na}_v1.3$ .

A number of studies have implicated upregulated  $\text{Na}_v1.3$  in the hyperexcitability of dorsal root ganglion neurons after injury (Black et al. 1999; Cummins and Waxman 1997; Kim et al. 2001), although one recent study questions the role of  $\text{Na}_v1.3$  in pain after nerve injury (Lindia et al. 2005). Our results are not directly comparable with the results of this study, however, because of differences in pain models,  $\text{Na}_v1.3$  AS sequences and tissue penetrability, and  $\text{Na}_v1.3$  antibodies used for protein detection. We previously showed that hyperresponsiveness of lumbar dorsal horn nociceptive neurons is associated with pain-related behavior after SCI and demonstrated the contribution of injury-induced upregulated expression of  $\text{Na}_v1.3$  (Hains et al. 2003b). In a study on pathological changes within the thalamus after SCI, more recently we showed that VPL neurons become hyperresponsive and produce afterdischarges to peripheral stimulation, develop larger peripheral receptive fields, and produce high rates of spontaneous activity that are independent of ascending spinal barrage; furthermore, we observed that these changes are associated with upregulated  $\text{Na}_v1.3$  (Hains et al. 2005).

Burst activity of VPL neurons was observed both in intact animals and in animals after SCI, but occurred more frequently after SCI. It has been hypothesized that bursts are involved in normal and pathological perceptual processing (for review, see Steriade 2004); however, rhythmic oscillation of burst firing is observed in pathophysiological conditions, and it has been suggested that abnormal thalamic activity may contribute to the perception of chronic pain (Jeanmonod et al. 1993; Lenz et al. 1989, 1994; see McCormick 1999).

Our data do not allow us to know what information is contained within normal or pathological bursts, but it has been suggested that the information content of bursts is higher than that for single spikes in the visual system (Reinagel et al. 1999), and the overall probability of generating at least one postsynaptic spike is higher for bursts than for single spikes in the hippocampus (Csicsvari et al. 1998). In neurons of the ventrobasal thalamus, increased gain or "transfer ratio" induced by burst firing results in increased thalamocortical efficacy, enhancing the postsynaptic response (Swadlow and Gusev 2001). Thus it is possible that pathological burst firing after SCI may more potently activate cortical circuits involved in pain perception.

In humans with post-SCI chronic pain, thalamic neurons exhibit oscillatory burst firing characterized by high discharge rates and deceleration of firing rate throughout the burst period (Lenz et al. 1989). Neurons in anesthetic zones and zones with intact sensory fields of the human thalamus show differential bursting activity after SCI, whereby burst activity in anesthetic zones occurred at higher frequencies than zones with intact sensory fields (Lenz et al. 1994). This may be attributable in part to deafferentation of the thalamus, raising the possibility that the emergence of an imbalance between thalamic nuclei contributes to neurogenic pain (Jeanmonod et al. 1993). One report, however, showed no correlation between bursting activity of thalamic neurons and pain (Radhakrishnan et al. 1999).

Our results are similar to those presented by Gerke et al. (2003), but we extend their data to show that, after SCI, burst firing intervals become more regular, spike events are reduced within each burst, acceleration in burst duration occurs in bursts containing higher spike counts, and shifts occur among spike firing modes. Furthermore, we observed that  $Na_v1.3$  AS returned the number of spikes/burst, burst duration, and inter-burst interval toward control levels after SCI. We cannot exclude, however, the additional potential contributions of other voltage-dependent ionic channels, such as calcium channels (Llinas and Jahnsen 1982), in configuring these electrophysiological changes.

The single-spike and burst events recorded in SCI animals are consistent with high-threshold calcium spikes (Guido et al. 1992; Jahnsen and Llinas 1984a,b; Llinas and Jahnsen 1982), although to a lesser extent, we also observed low threshold spikes. Changes in sodium current properties associated with  $Na_v1.3$  expression may, in turn, influence high-threshold calcium spikes, but the present results do not permit us to firmly make this conclusion. The ability of abnormally expressed  $Na_v1.3$  channels to generate rapidly inactivating currents at relatively negative potentials, as well as large ramp currents in response to slow depolarizations, suggest that neurons expressing  $Na_v1.3$  may exhibit a reduced threshold and/or a relatively high frequency of firing (Cummins et al. 2001). The biophysical properties of  $Na_v1.3$  may also contribute to lowered membrane potentials that configure neurons to transition from single-spike to burst firing in a voltage-dependent manner (Llinas and Jahnsen 1982).

Spindle waves, synchronized oscillations in thalamocortical and thalamic reticular systems typically observed during sleep and epilepsy, have also been associated with pain (Walker and Yaksh 1986). Damage to the spinal cord increases sleep spindle incidence in humans (Cicirata et al. 1983). Our recordings after SCI show an increased density of spindle waves compared with intact animals. Sodium currents play a role in spindle wave generation, specifically the plateau potentials and slow afterhyperpolarization that follow the cessation of each spindle wave (Kim and McCormick 1998), and it is possible that the altered kinetics conferred by  $Na_v1.3$  may influence spindle wave generation. Furthermore, because corticothalamic neurons participate in the generation of spindle waves, increased cortical activity associated with SCI (Hofstetter et al. 2003; Turner et al. 2003) may result in increased drive to thalamic reticular neurons that trigger spindle waves in thalamocortical neurons. Certain anesthetics can influence the frequency of spindle wave discharges, with barbiturates producing very strong spindles and halothane producing less-frequent occurrence. We used 1.1% halothane as a maintenance concentration for all of our recordings. It is known that halothane can depress the responses of dorsal horn WDR neurons to innocuous and noxious stimuli (Namiki et al. 1980; Yamauchi et al. 2002). Despite this caveat, halothane has been used extensively as an anesthetic for electrophysiological recording, particularly in the analysis of VPL neurons in the context of pain (Guilbaud et al. 1990).

This is the first study that examines abnormal thalamic activity after SCI in relation to the expression of  $Na_v1.3$ , and the mitigation of firing abnormalities by knockdown of  $Na_v1.3$ . Because the thalamus is involved in not only relaying but also processing incoming information from the spinal cord en route

to the cortex (see Lenz et al. 2004; Sherman and Guillery 2002), injury-induced changes in spinal pain generator circuitry may feed aberrant signals into the injured thalamus, which further processes and amplifies the signals before relaying to suprachiasmatic structures (Waxman and Hains 2006). Abnormal processing at thalamic levels would then be expected to further exaggerate abnormal firing patterns from the spinal cord after SCI. Our observations of increased primary burst firing activity and reduced silence in VPL neurons after SCI lead us to suggest that, after SCI, an increased level of abnormal afferent firing is being forwarded to cortical structures involved in interpreting pain. To further discriminate between dorsal horn and VPL effects, intracerebroventricular or direct administration of  $Na_v1.3$  AS into the VPL could be valuable.

Interruption of thalamic afferents has been suggested to contribute to changes in thalamic firing properties and chronic pain (Faggin et al. 1997; Jain et al. 1998; Weng et al. 2000), but thalamic abnormalities observed in our study cannot be explained solely by deafferentation of ascending inputs. In all of our analyzed units, the ability to elicit evoked responses by stimulation of the neuron's peripheral receptive field was a necessary requirement. It is quite possible, however, that in addition to  $Na_v1.3$  upregulation, reconfiguration of inputs or disinhibition of previously silenced inputs could contribute to penetration of subthreshold inputs that might alter burst firing properties (Ferreira-Gomes et al. 2004). Rhythmic network oscillation in the thalamus is accessible to external synaptic input and it has been shown that somatosensory afferents interact with other ascending pathways and corticothalamic projections (Muthuswamy et al. 1999). During sensory processing,  $\gamma$ -aminobutyric acid type B ( $GABA_B$ ) receptor-mediated inhibition seems to be important in modulating receptive field size of thalamic neurons, therefore regulating the efficacy of the sensory input (Lee et al. 1994). En passant axons of thalamocortical, as well as corticothalamic relay, neurons receive tuning from the surrounding nucleus reticularis feedback circuit, by a  $GABA_B$ ergic mechanism (Cox et al. 1997) that could be reconfigured after SCI.

In conclusion, our data show that after SCI, neurons of the VPL that possess well-defined peripheral receptive fields undergo alterations in a number of burst firing properties, and that  $Na_v1.3$  sodium channel is associated with these changes. We suggest that the abnormal burst firing of VPL neurons contributes to chronic neuropathic pain after SCI. It is unclear what effects abnormal burst firing have on higher-order cortical structures involved in pain perception. Further study of burst properties using techniques such as information transfer analysis and stimulus reconstruction (Reinagel and Reid 2000; Reinagel et al. 1999) could be helpful in deciphering the information content and significance of burst firing after SCI.

#### ACKNOWLEDGMENTS

The authors thank Dr. Joel Black for valuable experimental advice and B. Toftness for technical assistance.

#### GRANTS

This work was supported in part by grants from the Medical Research Service and Rehabilitation Research Service, Department of Veterans Affairs, and the National Multiple Sclerosis Society. The Center for Neuroscience and Regeneration Research is a collaboration of the Paralyzed Veterans of America and the United Spinal Association. B. C. Hains was funded by The Christopher

Reeve Paralysis Foundation (HB1-0304-2), National Institute of Neurological Disorders and Stroke Grant 1 F32 NS-046919-01, and Pfizer (Scholar's Grant in Pain Medicine).

## REFERENCES

- Altschul SF, Gish W, Miller W, Myers EW, and Lipman DJ. Basic local alignment search tool. *J Mol Biol* 215: 403–410, 1990.
- Apkarian AV, Sosa Y, Sonty S, Levy RM, Harden RN, Parrish TB, and Gitelman DR. Chronic back pain is associated with decreased prefrontal and thalamic gray matter density. *Neuroscience* 17: 10410–10415, 2004.
- Black JA, Cummins TR, Plumpton C, Chen YH, Hormuzdiar W, Clare JJ, and Waxman SG. Upregulation of a silent sodium channel after peripheral, but not central, nerve injury in DRG neurons. *J Neurophysiol* 82: 2776–2785, 1999.
- Cicirata F, Scrofanì A, Biondi R, and Papale A. Spindle activity during sleep in subjects with a deficit in pallesthetic sensibility. *Boll Soc Ital Biol Sper* 59: 1357–1363, 1983.
- Cox CL, Huguenard JR, and Prince DA. Nucleus reticularis neurons mediate diverse inhibitory effects in thalamus. *Proc Natl Acad Sci USA* 94: 8854–8859, 1997.
- Csicsvari J, Hirase H, Czurko A, and Buzsáki G. Reliability and state dependence of pyramidal cell-interneuron synapses in the hippocampus: an ensemble approach in the behaving rat. *Neuron* 21: 179–189, 1998.
- Cummins TR, Aglieco F, Renganathan M, Herzog RI, Dib-Hajj SD, and Waxman SG. Nav1.3 sodium channels: rapid repriming and slow closed-state inactivation display quantitative differences after expression in a mammalian cell line and in spinal sensory neurons. *Neuroscience* 21: 5952–5961, 2001.
- Cummins TR and Waxman SG. Down-regulation of tetrodotoxin-resistant sodium currents and up-regulation of a rapidly repriming tetrodotoxin-sensitive sodium current in small spinal sensory neurons following nerve injury. *Neuroscience* 17: 3503–3514, 1997.
- Faggini BM, Nguyen KT, and Nicoletis MA. Immediate and simultaneous sensory reorganization at cortical and subcortical levels of the somatosensory system. *Proc Natl Acad Sci USA* 94: 9428–9433, 1997.
- Ferreira-Gomes J, Neto FL, and Castro-Lopes JM. Differential expression of GABA(B1b) receptor mRNA in the thalamus of normal and monoarthritic animals. *Biochem Pharmacol* 68: 1603–1611, 2004.
- Gerke MB, Duggan AW, Xu L, and Siddall PJ. Thalamic neuronal activity in rats with mechanical allodynia following contusive spinal cord injury. *J Neurosci Methods* 117: 715–722, 2003.
- Gruner JA. A monitored contusion model of spinal cord injury in the rat. *J Neurotrauma* 9: 123–126, 1992.
- Guido W, Lu SM, and Sherman SM. Relative contributions of burst and tonic responses to the receptive field properties of lateral geniculate neurons in the cat. *J Neurophysiol* 68: 2199–2211, 1992.
- Guilbaud G, Benoist JM, Jazat F, and Gautron M. Neuronal responsiveness in the ventrobasal thalamic complex of rats with an experimental peripheral mononeuropathy. *J Neurophysiol* 64: 1537–1554, 1990.
- Hains BC, Eaton MJ, Willis WD, and Hulsebosch CE. Engraftment of serotonergic precursors amends hyperexcitability of dorsal horn neurons after spinal hemisection-induced central sensitization. *J Neurosci Methods* 116: 1097–1110, 2003a.
- Hains BC, Klein JP, Saab CY, Craner MJ, Black JA, and Waxman SG. Upregulation of sodium channel Nav1.3 and functional involvement in neuronal hyperexcitability associated with central neuropathic pain after spinal cord injury. *Neuroscience* 23: 8881–8892, 2003b.
- Hains BC, Saab CY, Klein JP, Craner MJ, and Waxman SG. Altered sodium channel expression in second-order spinal sensory neurons contributes to pain after peripheral nerve injury. *Neuroscience* 24: 4832–4839, 2004.
- Hains BC, Saab CY, and Waxman SG. Changes in electrophysiologic properties and sodium channel Na<sub>v</sub>1.3 expression in thalamic neurons after spinal cord injury. *Brain* 128: 2359–2371, 2005.
- Hains BC, Yucra JA, and Hulsebosch CE. Selective COX-2 inhibition with NS-398 preserves spinal parenchyma and attenuates behavioral deficits following spinal contusion injury. *J Neurotrauma* 18: 409–423, 2001.
- Hofstetter CP, Schweinhardt P, Klason T, Olson L, and Spenger C. Numb rats walk—a behavioural and fMRI comparison of mild and moderate spinal cord injury. *Eur J Neurosci* 18: 3061–3068, 2003.
- Hulsebosch CE, Xu GY, Perez-Polo JR, Westlund KN, Taylor CP, and McAdoo DJ. Rodent model of chronic central pain after spinal cord contusion injury and effects of gabapentin. *J Neurotrauma* 17: 1205–1217, 2000.
- Jahnson H and Llinas R. Electrophysiological properties of guinea-pig thalamic neurones: an in vitro study. *J Physiol* 349: 205–226, 1984a.
- Jahnson H and Llinas R. Ionic basis for the electro-responsiveness and oscillatory properties of guinea-pig thalamic neurones in vitro. *J Physiol* 349: 227–247, 1984b.
- Jain N, Florence SL, and Kaas JH. Reorganization of somatosensory cortex after nerve and spinal cord injury. *News Physiol Sci* 13: 143–149, 1998.
- Jeanmonod D, Magnin M, and Morel A. Thalamus and neurogenic pain: physiological, anatomical, and clinical data. *Neuroreport* 4: 475–478, 1993.
- Kim CH, Oh Y, Chung JM, and Chung K. The changes in expression of three subtypes of TTX sensitive sodium channels in sensory neurons after spinal nerve ligation. *Mol Brain Res* 95: 153–161, 2001.
- Kim U and McCormick DA. Functional and ionic properties of a slow afterhyperpolarization in ferret perigeniculate neurons in vitro. *J Neurophysiol* 80: 1222–1235, 1998.
- Lee SM, Friedberg MH, and Ebner FF. The role of GABA-mediated inhibition in the rat ventral posterior medial thalamus. I. Assessment of receptive field changes following thalamic reticular nucleus lesions. *J Neurophysiol* 71: 1702–1715, 1994.
- Lenz FA, Kwan HC, Dostrovsky JO, and Tasker RR. Characteristics of the bursting pattern of action potentials that occurs in the thalamus of patients with central pain. *Brain Res* 496: 357–360, 1989.
- Lenz FA, Kwan HC, Martin R, Tasker R, Richardson RT, and Dostrovsky JO. Characteristics of somatotopic organization and spontaneous neuronal activity in the region of the thalamic principal sensory nucleus in patients with spinal cord transection. *J Neurophysiol* 72: 1570–1587, 1994.
- Lenz FA, Weiss N, Ohara S, Lawson C, and Greenspan JD. The role of the thalamus in pain. *Suppl Clin Neurophysiol* 57: 50–61, 2004.
- Lindia JA, Kohler MG, Martin WJ, and Abbadié C. Relationship between sodium channel Na(V)1.3 expression and neuropathic pain behavior in rats. *Pain* 117: 145–153, 2005.
- Llinas R and Jahnsen H. Electrophysiology of mammalian thalamic neurones in vitro. *Nature* 297: 406–408, 1982.
- Loubser PG and Donovan WH. Diagnostic spinal anaesthesia in chronic spinal cord injury pain. *Paraplegia* 29: 25–36, 1991.
- McCormick DA. Are thalamocortical rhythms the Rosetta Stone of a subset of neurological disorders? *Nat Med* 5: 1349–1351, 1999.
- Melzack R and Loeser JD. Phantom body pain in paraplegics: evidence for a central “pattern generating mechanism” for pain. *Pain* 4: 195–210, 1978.
- Muthuswamy J, Tran P, Rangarajan R, Lenz FA, Hanley DF, and Thakor NV. Somatosensory stimulus entrains spindle oscillations in the thalamic VPL nucleus in barbiturate anesthetized rats. *Neurosci Lett* 262: 191–194, 1999.
- Namiki A, Collins JG, Kitahata LM, Kikuchi H, Homma E, and Thalhammer JG. Effects of halothane on spinal neuronal responses to graded noxious heat stimulation in the cat. *Anesthesiology* 53: 475–480, 1980.
- Pattany PM, Yezierski RP, Widerström-Noga EG, Bowen BC, Martinez-Arizala A, Garcia BR, and Quencer RM. Proton magnetic resonance spectroscopy of the thalamus in patients with chronic neuropathic pain after spinal cord injury. *Am J Neuroradiol* 23: 901–905, 2002.
- Paxinos G and Watson C. *The Rat Brain in Stereotaxic Coordinates* (4th ed.). San Diego, CA: Academic Press, 1998.
- Price DD and Dubner R. Neurons that subserve the sensory-discriminative aspects of pain. *Pain* 3: 307–338, 1977.
- Radhakrishnan V, Tsoukatos J, Davis KD, Tasker RR, Lozano AM, and Dostrovsky JO. A comparison of the burst activity of lateral thalamic neurons in chronic pain and non-pain patients. *Pain* 80: 567–575, 1999.
- Reinagel P, Godwin D, Sherman SM, and Koch C. Encoding of visual information by LGN bursts. *J Neurophysiol* 81: 2558–2569, 1999.
- Reinagel P and Reid RC. Temporal coding of visual information in the thalamus. *Neuroscience* 20: 5392–5400, 2000.
- Sherman SM and Guillery RW. The role of the thalamus in the flow of information to the cortex. *Philos Trans R Soc Lond B Biol Sci* 357: 1695–1708, 2002.
- Steriade M. Neocortical cell classes are flexible entities. *Nat Rev Neurosci* 5: 121–134, 2004.

- Swadlow HA and Gusev AG.** The impact of “bursting” thalamic impulses at a neocortical synapse. *Nat Neurosci* 4: 402–408, 2001.
- Turner JA, Lee JS, Schandler SL, and Cohen MJ.** An fMRI investigation of hand representation in paraplegic humans. *Neurorehabil Neural Repair* 17: 37–47, 2003.
- Walker GE and Yaksh TL.** Studies on the effects of intrathalamically injected DADL and morphine on nociceptive thresholds and electroencephalographic activity: a thalamic delta receptor syndrome. *Brain Res* 383: 1–14, 1986.
- Waxman SG and Hains BC.** Fire and phantoms after spinal cord injury: Na(+) channels and central pain. *Trends Neurosci* 2006 Feb 20 [Epub ahead of print].
- Weng HR, Lee JI, Lenz FA, Schwartz A, Vierck C, Rowland L, and Dougherty PM.** Functional plasticity in primate somatosensory thalamus following chronic lesion of the ventral lateral spinal cord. *J Neurosci Methods* 101: 393–401, 2000.
- Willis WD and Coggeshall RE.** *Sensory Mechanisms of the Spinal Cord* (3rd ed.). New York: Plenum Press, 2004.
- Yamauchi M, Sekiyama H, Shimada SG, and Collins JG.** Halothane suppression of spinal sensory neuronal responses to noxious peripheral stimuli is mediated, in part, by both GABA(A) and glycine receptor systems. *Anesthesiology* 97: 412–417, 2002.